Supplemental Information

Neutron diffraction of acetazolamide-bound human carbonic anhydrase II reveals atomic details of drug binding

[1]S. Zoë Fisher, [2]Mayank Aggarwal, [1]Andrey Y. Kovalevsky, [3]David N. Silverman, [2*]Robert McKenna

[1]Bioscience Division, Los Alamos National Laboratory, Los Alamos NM 87545; [2]Department of Biochemistry and Molecular Biology, PO Box 100245, University of Florida, Gainesville 32610; [3]Department of Pharmacology and Therapeutics, PO Box 100247, University of Florida, Gainesville FL 32610.

- Corresponding author: Robert McKenna: rmckenna@ufl.edu (352) 392-5696

Experimental

HCA II expression and purification

HCA II was expressed in BL21 DE3* pLysS *E.coli*. The cells were grown in autoinduction LB Express media (Novagen) for 16 hours with 1mM $ZnSO_4$ and 0.1 mg/mL Ampicillin added at the time of inoculation. Cells were harvested by centrifugation at 5000 rpm and lysed by sonication on ice. The resulting cell lysate was clarified by spinning at 9500 rpm for 90 minutes prior to loading onto pAMBS resin (Sigma Aldrich). Unbound proteins and nucleic acids were removed by repeated wash steps with buffer A (0.2 M Na_2SO_4, 100 mM Tris pH 9.0) and buffer B (0.2 M Na_2SO_4, 100 mM Tris pH 7.0). Bound HCA II was eluted with 50 mM Tris pH 7.8 and 0.4 M NaN_3. The eluted protein was concentrated with Amicon Ultra concentration devices (10 kDa molecular weight cut off) and buffer-exchanged into 50 mM Tris pH 8.0 by dialysis.

HCA II and AZM co-crystallization

Purified HCA II was concentrated to 35 mg/mL before mixing with 10 mM AZM (American Cynamid Company, Batch No. X5540). The complex was allowed to incubate at room temperature for 30 minutes. Any precipitation was removed by centrifugation prior to crystallization drop set-up. Sitting drop crystallization of HCA II:AZM was carried out using the sandwich box set-up from Hampton Research. Using these large trays facilitates large crystal growth as drop sizes can approach 1mL. In this case 400 μL crystallization drops were set up in siliconized glass plates by mixing 200 μL of well solution (1.3 M sodium citrate, 0.1 M Tris pH 9.0) with 200 μL of the HCA II:AZM complex against 25 mL of mother liquor. This set-up is allowed to equilibrate in a 20 ºC incubator for 7-10 days. At this point sodium citrate salt is added to the well until it reaches saturation and re-crystallizes. Crystals typically take 2-4 weeks to grow to maximal size.

Neutron and X-ray diffraction data collection

A large single crystal (~2 mm^3 volume) was mounted in a quartz capillary (Figure

S1), with D_2O mother liquor placed at one end of the capillary prior to sealing. The crystal was left to undergo H/D exchange for ~4 weeks before data collection was started. Bennett *et al.* reported that most labile H atoms are exchanged by D atoms fairly rapidly with ~80% amide backbone exchange happening in about a month (Bennet *et al.*, 2008). The crystal was ransported to the Protein Crystallography Station (PCS) for neutron data collection. Time-of-flight, wavelength-resolved neutron Laue diffraction images were collected at room temperature. The sample was mounted on a Huber κ-circle goniometer and 33 settings were recorded on the position sensitive ^{3}He-filled neutron detector. Each frame corresponds to 16h exposure and corresponds to 22 days total beam time.

Each image was processed using a version of d*TREK (Pflugrath, 1999) modified for wavelength-resolved Laue neutron protein crystallography (Langan & Greene, 2004). The integrated reflections were wavelength normalized using LAUENORM (Helliwell *et al.*, 1989; Cruickshank, 1999) and then merged using SCALA incorporated into the CCP4i (Evans, 2005; Diederichs & Karplus, 1997; Weiss & Hilgenfeld, 1997; Collaborative Computational Project Number 4, 1994). The wavelength range was restricted to 0.6-6.2 Å so as to eliminate the least accurately measured reflections. The overall completeness was ~86% to 2.0 Å, with an R_{sym} of ~ 26% and redundancy of 3.2 (Table S1).

A room temperature X-ray diffraction data set was collected from a similar crystal from the same drop. This crystal was also subjected to in-capillary H/D exchange prior to data collection. Data were collected on an in-house Rigaku HighFlux home source equipped with 007 Micromax optics and an R-AXIS IV++ image plate. The source was a Cu rotating anode operated at 40 kV and 30 mA (Table 1). The crystal-detector distance was 100 mm and the oscillation steps were 0.5° with a 2 minute exposure per frame. Data processing and reduction were done using HKL3000 (Minor *et al.*, 2006). X-ray data was collected to 1.6 Å resolution from 240 frames. The data set statistics are shown in Table 1.

Joint X-ray and neutron structure refinement

Refinement of the model against X-ray data was completed first using *PHENIX* (Adams *et al.*, 2010). The starting model was derived from PDB ID 3hs4 after removing

Zn, solvent, and the AZM coordinates (Sippel *et al.*, 2009). After convergence of the X-ray crystallographic R factors, H atoms and D atoms - at labile positions - were generated and the joint refinement was moved into *nCNS* (Mustyakimov and Langan, 2007; Adams *et al.*, 2009). This version of CNS has been modified for joint X-ray and neutron refinement where two structure factor files are read in and one model is refined against both data sets. Joint refinement included iterative rounds of positional, individual B factor, and occupancy refinement. Based on Visual inspection of nuclear and electron density $2F_o$-F_c and F_o-F_c maps allowed for the placement of AZM, Zn, and D_2O molecules as well as the identification of the protonation states of amino acid side chains such as His. In cases where the neutron data was not definitive, H/D atoms and solvent were oriented to accommodate H-bonds and electrostatic interactions. All manual model building was done using Coot (Emsley and Cowtan, 2004) and figures were generated with PyMOL (Delano, 2002). The final model was refined to R_{cryst}/R_{free} of 26.8/28.3 and 17.4/18.9 for neutron and X-data, respectively. The model contains 166 D_2O molecules and r.m.s. deviation for bond lengths (Å) and angles (°) are 0.01 and 1.4, respectively. Table 1 shows a summary of the refinement statistics. Model coordinates and neutron experimental data have been deposited with the RCSB Protein Data Bank, with accession code 4goc.

References

Adams, P. D., Mustyakimov, M., Afonine, P. V. & Langan, P. Generalized X-ray and neutron crystallographic analysis: more accurate and complete structures for biological macromolecules. *Acta Cryst.* **2009**, *D65*, 567-573.

Adams, P.D., Afonine, P.V., Bunkoczi, G., Chen, V.B., Davis, I.W., Echols, N., Headd, J.J., Hung, L.-W., Parkal. G.J., Grosse-Kunstleve, R.W., McCoy, A.J., Moriarty, N.W., Oeffner, R., Read, R.J., Richardson, D.C., Richardson, J.S., Terwilliger, T.C., Zwart, P.H. PHENIX: a comprehensive Python-based system for macromolecular structure solution. *Acta Cryst.* **2010**, *D66*, 213-221.

Bennett, B.C., Gardberg, A.S., Blair, M.D., Dealwis, C.G. On the determinants of amide backbone exchange in proteins: a neutron crystallographic comparative study. *Acta Cryst.* **2008**, *D64*, 764-783.

Collaborative Computational Project, Number 4. *Acta Cryst.*, **1994**, *D50*, p.760-763.

DeLano, W.L. The PyMOL Molecular Graphics System. **2002**, DeLano Scientific, San Carlos, CA, USA. http://www.pymol.org.

Cruickshank, D.W. Remarks about protein structure precision *Acta Cryst.*, **1999**, *D55*, p.583-601.

Diederichs, K., Karplus, P. A. Improved R-factors for diffraction data analysis in macromolecular crystallography. *Nat. Struct. Biol.* **1997**, *4*, p.269-275

Emsley, P., Cowtan, K. Coot: model-building tools for molecular graphics. *Acta Crystallogr.* **2004**, *D60*, p.2126-2132.

Evans, P. R. Scaling and assessment of data quality. *Acta Cryst.*, **2005**, *D62*, p.72-82.

2004, *D60*, p.2126-2132.

Helliwell, J. R., Habash, J., Cruickshank, D. W. J., Harding, M. M., Greenhough, T. J., Campbell, J. W., Clifton, I. J., Elder, M., Machin, P. A., Papiz, M. Z. & Zurek, S. The recording and analysis of synchrotron X-radiation Laue diffraction photographs. *J. Appl. Cryst.* **1989**, *22*, p.483-497.

Langan, P., Greene, G. Protein crystallography with spallation neutrons: collecting and processing wavelength-resolved Laue neutron data. *J. Appl. Cryst.*, 2004, *37*, p.253-257.

Minor, W., Cymborowski, M., Otwinowski, Z., Chruszcz, M. HKL-3000: the integration of data reduction and structure solution – from diffraction images to an initial model in minutes. *Acta Crystallogr.* **2006**, *D62*, p.859-866.

Mustyakimov, M, Langan, P. **2007**, Copyright C-06, 104 Patch for CNS; nCNS an Open source distribution patch for CNS for macromolecular structure refinement (download from http://mnc.lanl.gov).

Pflugrath, J. W. The finer things in X-ray diffraction data collection. *Acta Crystallogr.* **1999**, *D55*, p.1718-1725.

Sippel, K., Robbins, A.H., Domsic, J., Genis, C., Agbandje-McKenna, M., McKenna, R. High-resolution structure of human carbonic anhydrase II complexed with acetazolamide reveals insights into inhibitor drug design. *Acta Crystallogr.* **2009**, *F65*, p.992-995.

Weiss, M., Hilgenfeld, R. On the use of the merging R factor as a quality indicator for X-ray data. *J. Appl. Cryst.*, **1997**, *30*, p.203-205.

Table S1. Crystallographic data collection and refinement statistics. Values in parenthesis are for the highest resolution shell.

CA+AZM	RT X-ray	RT Neutron
Source	Rotating Cu Anode	LANSCE, PCS
Wavelength (Å)	1.54	0.6 – 6.2
Unit cell: *a, b, c, β* (Å, °)	42.8, 42.7, 72.9, 104.6	42.8, 42.7, 72.9, 104.6
Space group	$P2_1$	$P2_1$
Settings	240	33
Resolution (Å)	40 – 1.60 (1.66 – 1.60)	20.0 - 2.0 (2.11 - 2.00)
No. of unique reflections	31126 (2989)	14486 (1782)
Redundancy	5.1 (5.1)	3.2 (2.1)
Completeness (%)	93.6 (89.6)	85.7 (73.4)
Mean I/σ(I)	33.8 (20.0)	6.9 (2.1)
$^{\dagger}\mathbf{R_{p.i.m.}}$	N/A	14.9 (27.8)
$^{\S}\mathbf{R_{merge}}$	3.5 (8.5)	25.8 (39.2)
No. of atoms (incl H/D atoms): *main- , side-chain, water*	N/A	1029, 3030, 498
Ave. B factor (incl H/D atoms): *main-, side-chain, water*	N/A	15.3, 17.9, 43.5
JOINT $^{\int}\mathbf{R_{cryst}}$, $^{*}\mathbf{R_{free}}$	17.4, 18.9	26.8, 28.3

$^{\S}R_{merge} = (\Sigma \mid I - \langle I \rangle \mid / \Sigma \langle I \rangle) \times 100$

$^{\dagger}R_{p.i.m.} = (\Sigma [1/(N-1)]^{1/2} \Sigma \mid I - \langle I \rangle \mid / \Sigma\Sigma I) \times 100$

$^{\int}R_{cryst} = (\Sigma \mid F_O - F_C \mid / \Sigma \mid F_O \mid) \times 100$

*R_{free} is calculated in the same way as R_{cryst} for data omitted from refinement (5% of reflections for all data sets).

Figure S1. Stick representation of the active site of neutron structure of unbound HCA II (PDB 3tmj; Fisher *et al.*, 2011) showing well-ordered waters S1, S2, S3, and S4. AZM displaces the aforementioned water molecules to bind in the active site. Zn^{2+} is shown as a blue sphere. Figure was generated in PYMOL.

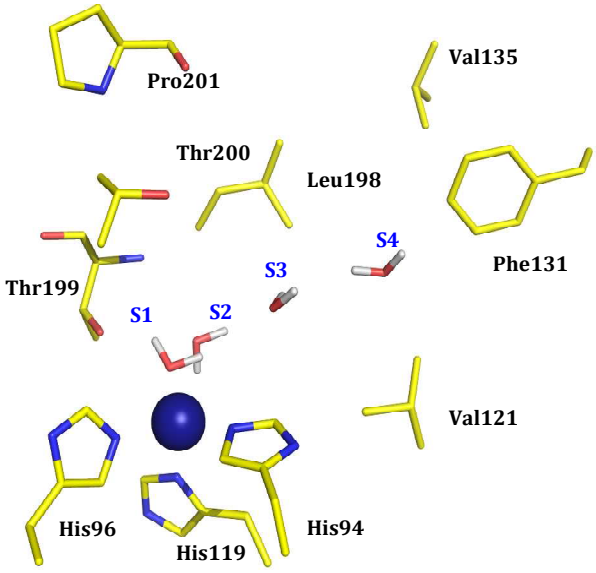

Figure S2. Active site of HCA II-AZM (yellow cartoon and sticks) and residues that are different residues in HCA IX are shown in green ball-and-stick (Val131 and Leu135). Coordinates were taken from PDB ID 3iai (Alterio *et al.*, 2009). Zn^{2+} is shown as a blue sphere. Figure was generated in PYMOL.